Electronic Supplementary Material (ESI) for Materials Advances.

Supporting information

The effect of ZnO particle lattice termination on the DC conductivity of LDPE nanocomposites

M. E. Karlsson,[a] A. Calamida,[a] D. Forchheimer,[b] H. Hillborg,[c] V. Ström,[d] J. M. Gardner,[e] M. S. Hedenqvist[a] and R. T. Olsson*[a]

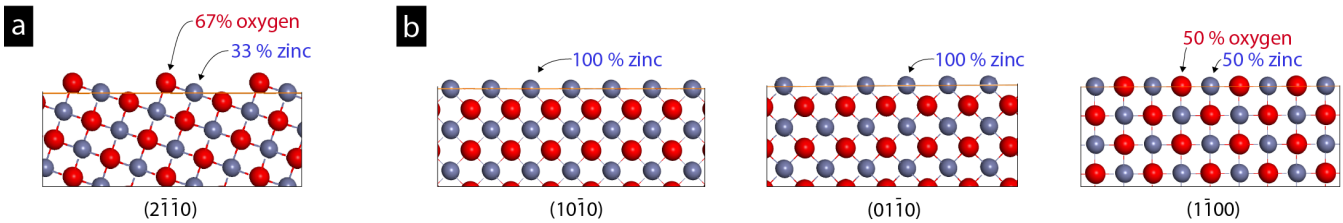

Fig. S1. Atomic surface terminations of zinc (blue) and oxygen (red) from the dominant crystal planes of (a) the sheets in the ball-shaped particles and (b) the sides of the rod-shaped particles illustrated by atomistic modelling.

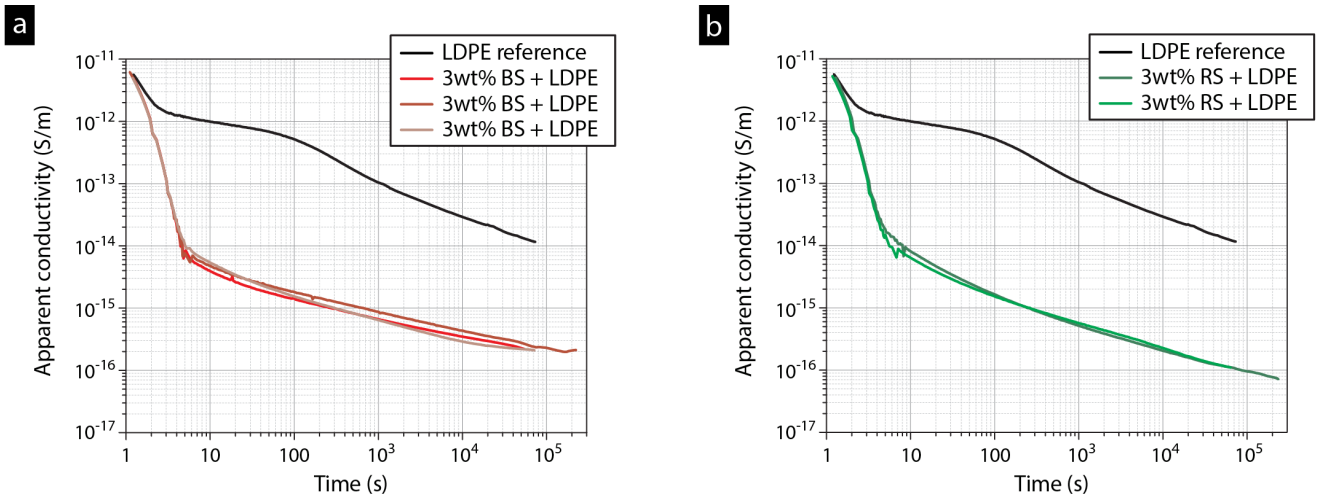

Fig. S2. DC conductivity measurements on composites containing 3 wt% of unmodified (a) ball-shaped particles and (b) rod-shaped particles.

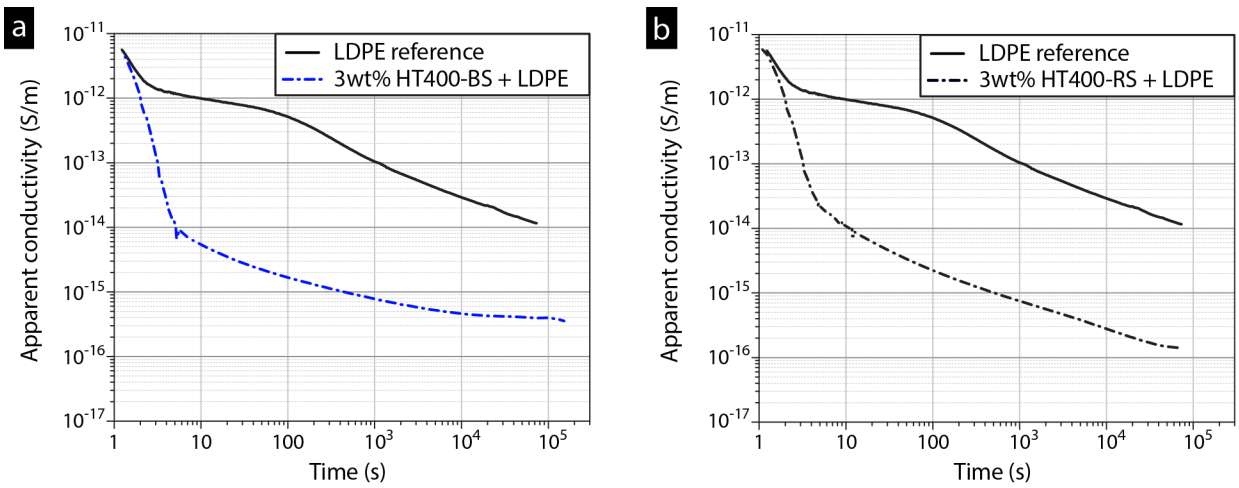

Fig. S3. DC conductivity measurements on composites containing (a) 3 wt% of heat-treated ball-shaped particles and (b) 3 wt% of heat-treated rod-shaped particles. The particles where heat-treated at 400 °C for 1 h in air prior to compounding with LDPE.

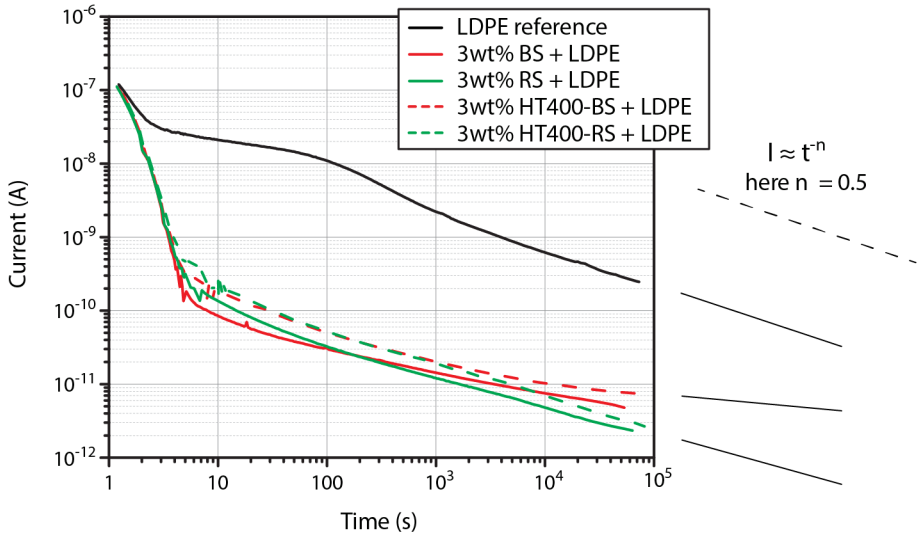

Fig. S4. Charging current at 60 °C with an electric field of 30 kV mm^{-1} for composites containing 3 wt% unmodified or heat treated (400 °C) ZnO particles in the shape of rods and balls. Extrapolation of composites with heat-treated particles and the LDPE reference is shown and compared to the power law expression $I \approx t^{-n}$, with n=0.5 (dotted line).

Table S1. DC conductivity, peak melting temperature (T_m), onset crystallization temperature (T_c) and mass crystallinity (w_c) of LDPE composites containing 3 wt% of ZnO particles.

Composite filler		Particle surface treatment	DC conductivity [b] (S m^{-1})	T_m (°C)	T_c (°C)	w_c [c] (%)
Particle size	Particle morphology					
- [a]	- [a]	- [a]	1.2×10^{-14}	110	102.5	51
micro	ball (interconnected sheets)	unmodified	2.4×10^{-16}	109.9	102.6	50
micro	ball (interconnected sheets)	heat treated at 400 °C	3.9×10^{-16}	110	102.7	53
micro	ball (interconnected sheets)	SiO_2	1.8×10^{-15}	109.9	102.2	52
micro	ball (interconnected sheets)	C8	9.5×10^{-17}	109.9	102.4	54
micro	rod	unmodified	1.2×10^{-16}	110.1	102.5	50
micro	rod	heat treated at 400 °C	1.5×10^{-16}	109.9	102.4	55
micro	rod	SiO_2	1.7×10^{-15}	109.8	102.1	55
micro	rod	C8	9.4×10^{-17}	110	102.3	54
nano	hexagonal pyramid	unmodified	3.5×10^{-17}	109.8	103	53
nano	hexagonal pyramid	SiO_2	4.7×10^{-16}	109.8	102.2	52
nano	hexagonal pyramid	C8	1×10^{-17}	110	104	54

[a] Pristine LDPE reference
[b] Apparent conductivity calculated with Eq. 2 after applied voltage for 15 h at 60 °C and 30 kV mm^{-1}.
[c] Mass crystallinity calculated with Eq. 1.

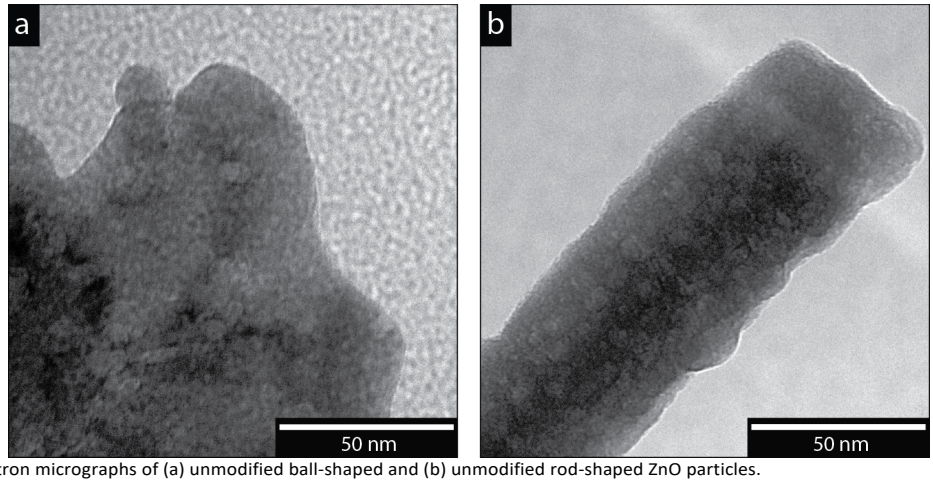

Fig. S5. Transmission electron micrographs of (a) unmodified ball-shaped and (b) unmodified rod-shaped ZnO particles.

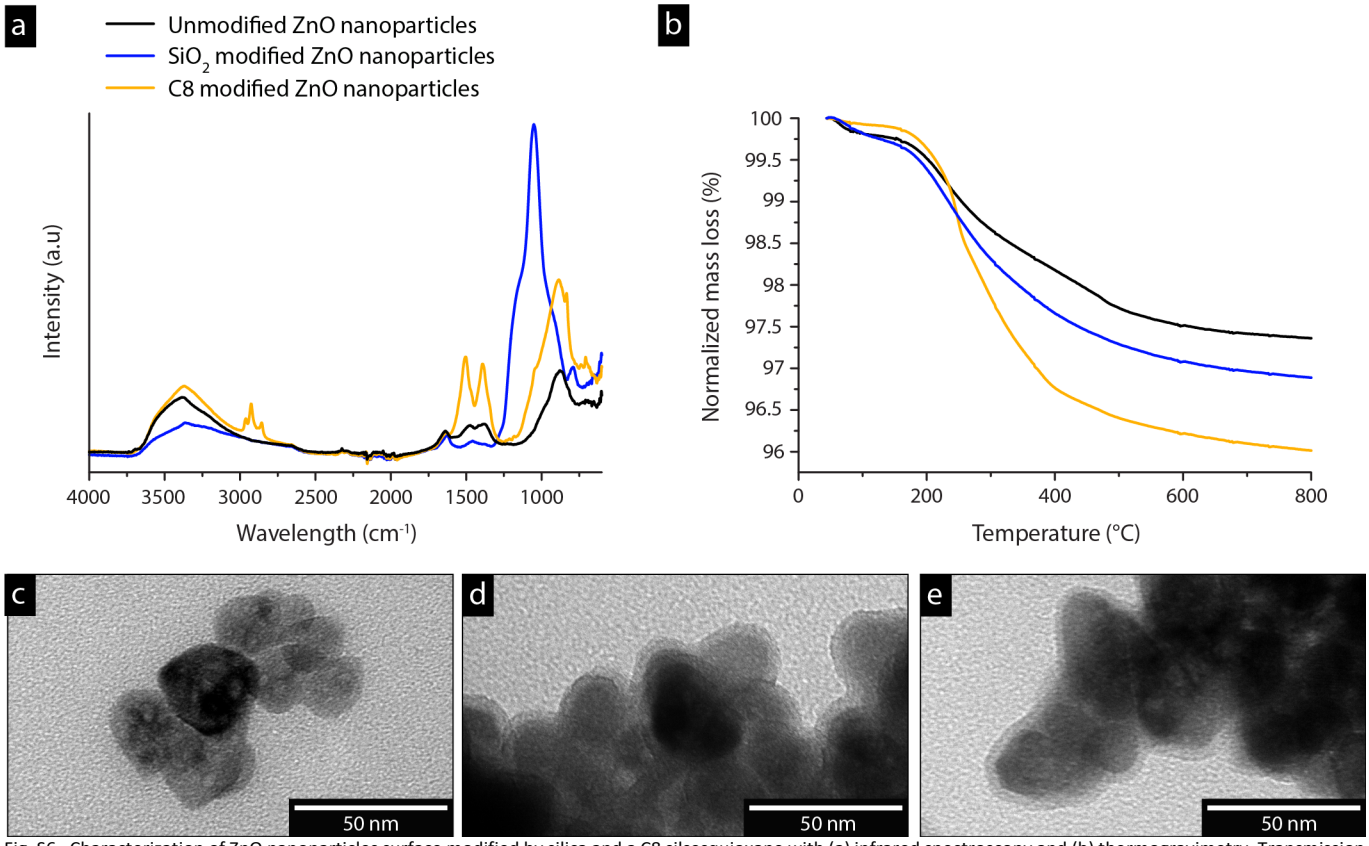

Fig. S6. Characterization of ZnO nanoparticles surface modified by silica and a C8 silsesquioxane with (a) infrared spectroscopy and (b) thermogravimetry. Transmission electron micrographs are shown in (c) for unmodified nanoparticles, (d) for silica modified nanoparticles and (e) for C8 modified nanoparticles.

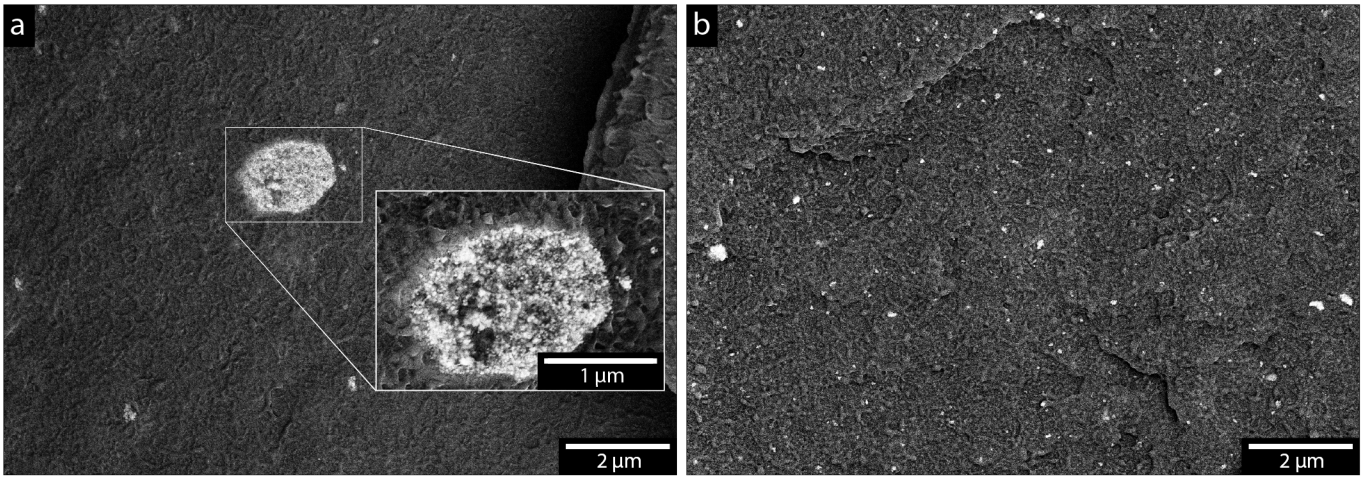

Fig. S7. Micrographs of (a) a LDPE composite containing 3 wt% unmodified ZnO nanoparticles, where a particle agglomerate larger than 1 µm is present (see inset), and (b) the dispersion of C8-coated ZnO nanoparticles in LDPE.

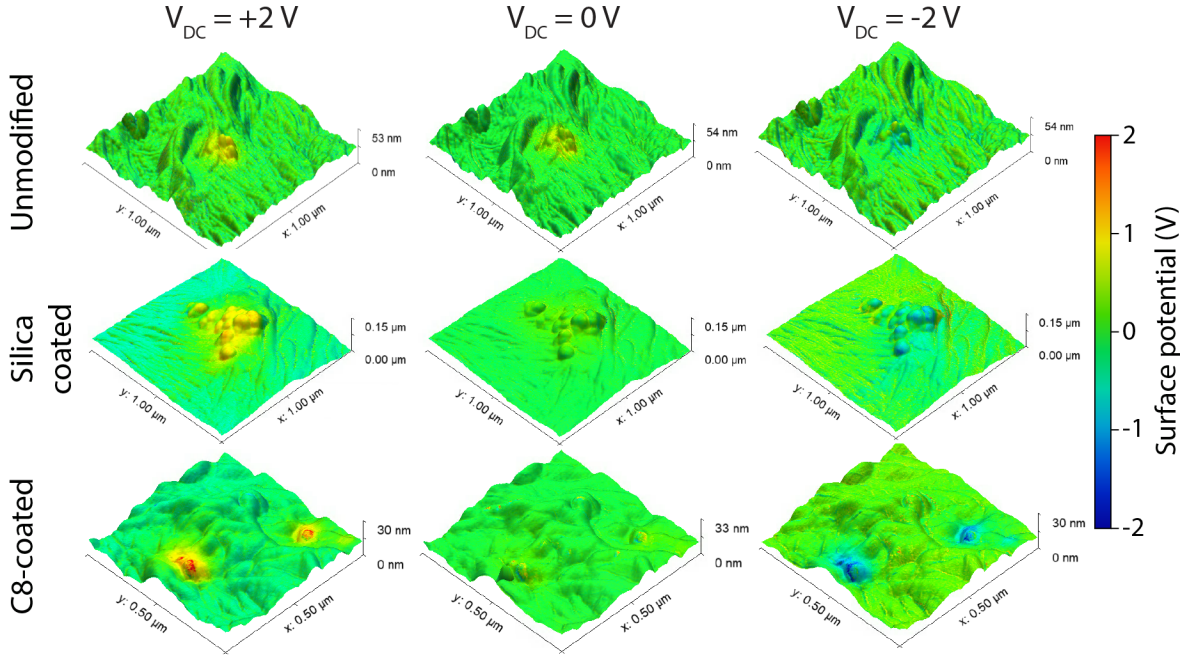

Fig. S8. Intermodulation electrostatic force microscopy of spin-coated 100 nm thick composite samples containing unmodified, silica coated or C8 surface modified ZnO nanoparticles, measured with a DC bias ($-2 \leq V_{DC} \leq 2$) between the tip and the surface.

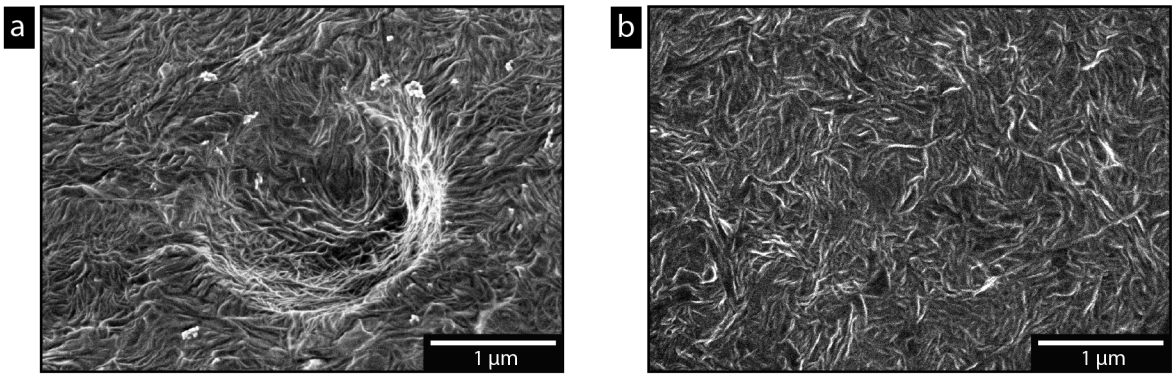

Fig. S9. Micrographs of the polyethylene crystalline structure in (a) a composite containing 3 wt% unmodified ball-shaped particles and (b) the LDPE reference revealed by etching the cross-section after freeze-cracking a thin film sample in liquid nitrogen.